Total Variation-Regularized Compressed Sensing Reconstruction for Multi-shell Diffusion Kurtosis Imaging

Jonathan I. Sperl[1], Tim Sprenger[1,2], Ek T. Tan[3], Vladimir Golkov[1,4], Marion I. Menzel[1], Christopher J. Hardy[3], and Luca Marinelli[3]
[1]*GE Global Research, Munich, BY, Germany,* [2]*IMETUM, Technical University Munich, Munich, BY, Germany,* [3]*GE Global Research, Niskayuna, NY, United States,*
[4]*Computer Vision Group, Technical University Munich, Munich, BY, Germany*

Introduction: In Diffusion Kurtosis Imaging (DKI) the data are sampled in a series of concentric shells in the diffusion encoding space (q-space) [1]. Typical DKI acquisition schemes consist of 5 shells with 30 directions per shell requiring 150 data points in total and a scan time in the order of 5 to 10 minutes. Reducing the number of acquired data points yields a linear reduction in scan time and may thereby improve the clinical applicability of DKI. Several methods have been proposed to accelerate the DKI acquisition by undersampling the multi-shell data and reconstructing the missing data points using compressed sensing (CS) [2-4]. These methods work by exploiting sparse signal representations *within a shell* using particular basis functions (spherical ridgelets, spherical polar Fourier bases etc.). In contrast to that, this work proposes to also make use of properties of the data *across shells*. Similar to the 3D Fourier relation between q-space and the diffusion propagator space (r-space) exploited in CS-accelerated Diffusion Spectrum Imaging (DSI) [5], the 1D Fourier relation between a radial line in q-space and its reciprocal space is used to reconstruct a bundle of 1D propagators which are regularized by a non-Cartesian total variation (TV) operator.

Theory: Assume a multi-shell diffusion acquisition where the data are sampled on spokes with an equidistant spacing in q (see Fig. 1, left) and characterized by the diffusion gradient strength q and spherical coordinates φ and ϑ. Exploiting symmetry in q-space, the data can be mirrored at the origin yielding a point-symmetric data set (Fig. 1, center). A 1D Fourier transform along each mirrored spoke in q-space yields a bundle of (real valued) 1D propagators in the (r, φ, ϑ)-space (Fig. 1, right).

The data in the (r, φ, ϑ)-space are also sampled on a series of shells and can be assumed to vary smoothly within each shell because typical propagators vary slowly with direction. This motivates the introduction of a non-Cartesian TV operator on a shell: Consider the set N_i of indices of J neighbors of the i-th spoke (φ_i, ϑ_i) in circular order around the spoke. A typical choice for the number of neighbors considered would be J=6, forming a hexagon around the spoke. Hence the root sum of the squared finite differences of the propagator bundle $p(r, \varphi, \vartheta)$ around the i-th spoke and the k-th shell reads

$$\mathrm{FD}_{k,i}(p) = \sqrt{\sum_{\substack{j\in N_i,\\ j\le J/2}} \left(\frac{p(r_k,\varphi_j,\vartheta_j) - p(r_k,\varphi_{J/2+j},\vartheta_{J/2+j})}{s_{i,j}+s_{iJ/2+j}} \right)^2} \qquad (1)$$

weighted by the distances $s_{i,j}$ between the i-th spoke and its j-th neighbor. Note that the indexing pairs j and $J/2+j$ in the left and right summands, respectively, are used to address neighbors lying opposite one another with respect to the center of the hexagon.

Hence the TV of the propagator p reads

$$\mathrm{TV}(p) = \sum_{i,k} \mathrm{FD}_{k,i}(p). \qquad (2)$$

The TV operator now serves as a regularizer in the following reconstruction task:

$$\min_p \|M\mathcal{F}p - d\|_2 + \lambda \mathrm{TV}(p), \qquad (3)$$

where d denotes the undersampled and mirrored q-space data, $\mathcal{F}$ the 1D Fourier transform, M the undersampling mask, and λ a scaling parameter. Equation (3) can be solved using an *Iterative Shrinkage/Thresholding Algorithm* (ISTA) [5-7] yielding an optimum propagator p_{opt}. Subsequently, the q-space signal (including the missing data points) can be recovered as $\mathcal{F}p_{\mathrm{opt}}$.

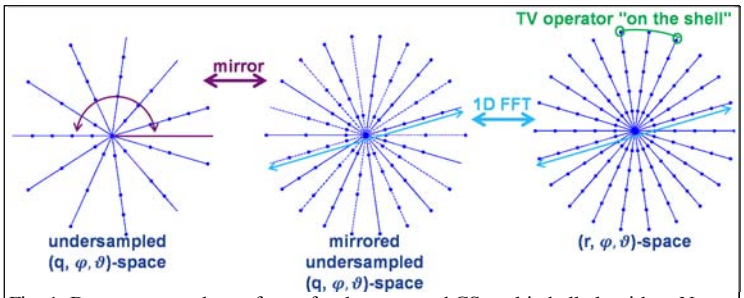

Fig. 1: Data spaces and transforms for the proposed CS-multi-shell algorithm. Note that this is a simplified 2D representation of the 3D scenario.

Methods: Experiments on a healthy volunteer were performed on a 3T GE MR750 clinical MR scanner (GE Healthcare, Milwaukee, WI, USA) using a 32-channel head coil (single shot EPI, single spin echo, *TE =84.3 ms, TR = 1.8 s, 96x96, FOV=24 cm*) and a 5-shell DKI acquisition with 30 directions per shell, equidistant sampling in q and b_{max} = *3,000 s/mm*^{2}. In addition, *b=0*-images were acquired every 20-th image and used for affine motion correction. In order to simulate accelerated acquisitions, the data were artificially undersampled using acceleration factors R=1.25, R=1.5, R=1.75, and R=2 (corresponding to 120, 100, 85, and 75 data points, respectively) and a series of 50 pattern instances per acceleration factor. The proposed CS-reconstruction was performed for all undersampled data sets. Additional diffusion MRI data of the same volunteer and identical imaging parameters, consisting of a 515 point DSI acquisition and another 150 point multi-shell acquisition, was combined with the fully sampled data and used as a "ground truth" data set. Using weighted linear least squares [8], diffusion and kurtosis tensors were fitted for the ground truth (GT), the fully sampled ($\mathrm{DKI}_{\mathrm{full}}$), the undersampled ($\mathrm{DKI}_{\mathrm{us}}$) and the CS-reconstructed ($\mathrm{DKI}_{\mathrm{CS}}$) data sets.

Typical diffusion and kurtosis metrics such as fractional anisotropy (FA), mean (K_{mean}), maximum (K_{max}), and orthogonal (K_{orth}) kurtosis were computed for all fitted tensors. Furthermore, the apparent kurtosis coefficient (AKC) was computed for 512 directions (isotropically distributed on the unit sphere) and its root mean squared error (RMSE) with respect to the GT was determined for every voxel.

Results: Fig. 2 depicts the RMSE(AKC) (averaged over all voxels) for all patterns. The error of $\mathrm{DKI}_{\mathrm{CS}}$ was always lower than for $\mathrm{DKI}_{\mathrm{us}}$ and up to R=1.75 even below the error of $\mathrm{DKI}_{\mathrm{full}}$. Fig. 3 shows the resulting kurtosis, RMSE(AKC) and FA maps for a single pattern at R=1.5. For $\mathrm{DKI}_{\mathrm{CS}}$, the kurtosis maps appear less noisy and have a better structural preservation compared to $\mathrm{DKI}_{\mathrm{us}}$ and partly even to $\mathrm{DKI}_{\mathrm{full}}$. Also the RMSE(AKC) is reduced and the FA map is slightly denoised.

Discussion: The proposed CS reconstruction method for multi-shell acquisitions allows acceleration of typical DKI acquisition by a factor of R=1.75 without significant loss in the quality of derived kurtosis metrics. Further investigations may compare this approach with ridgelet-based methods and extend the concept to more general DKI sampling schemes.

References: [1] Jensen *et al.*, NMR Biomed, 2010; [2] Michailovich *et al.*, IEEE TMI, 2011; [3] Rathi *et al.*, ISMRM Workshop Diffusion, Podstrana, Croatia, 2013; [4] Merlet, Med Image Anal, 2013; [5] Menzel *et al.*, MRM, 2011; [6] Donoho and Johnstone, JASA, 1995; [7] Sperl *et al.*, Proc. ISMRM 2012; [8] Veraart *et al.*, MRM, 2011.

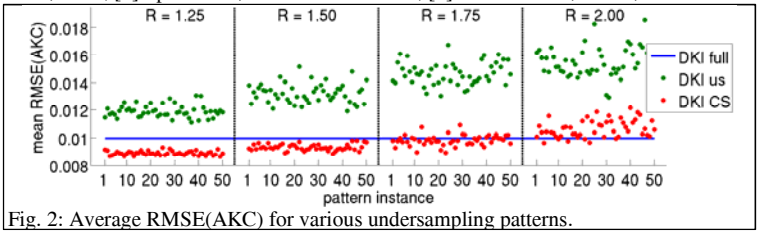

Fig. 2: Average RMSE(AKC) for various undersampling patterns.

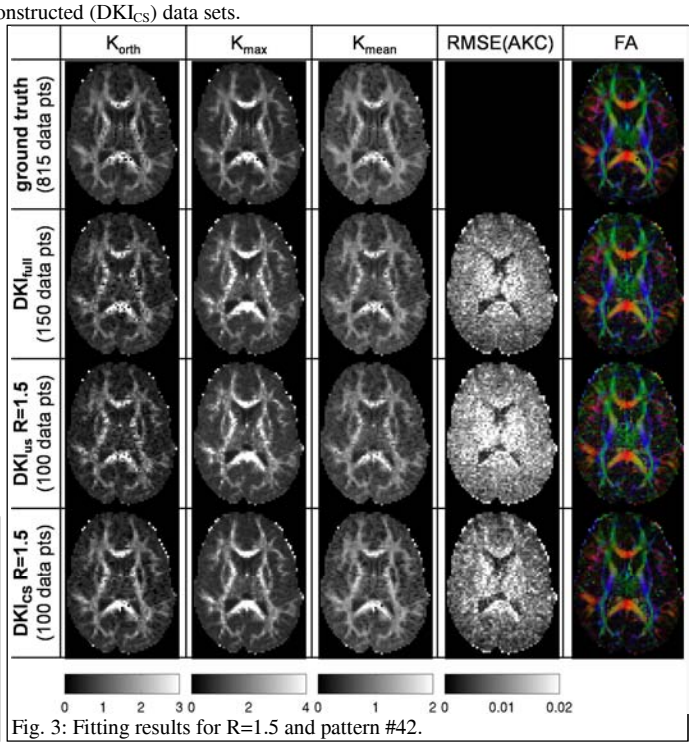

Fig. 3: Fitting results for R=1.5 and pattern #42.